Time-Resolved EPR Studies of Main Chain Radicals from Acrylic Polymers. Dynamic Effects Due to Conformational Motion

Vanessa P. McCaffrey, Elizabeth J. Harbron, and Malcolm D. E. Forbes*

Venable and Kenan Laboratories, Department of Chemistry, CB #3290, University of North Carolina, Chapel Hill, North Carolina 27599

Received October 25, 2004; Revised Manuscript Received February 9, 2005

ABSTRACT: The temperature dependencies of the time-resolved electron paramagnetic resonance (TREPR) spectra of five main chain acrylic free radicals are presented and discussed in terms of conformational dynamics. The radicals are produced in liquid solution at temperatures ranging from 25 °C to over 100 °C by direct excitation (248 nm) of the ester group in the polymers leading to Norrish I α-cleavage of the side chain ester moiety. Restricted rotational motion near the radical center leads to modulation of the β-hyperfine coupling constants, which manifests itself in some of the spectra as an alternating line width effect near room temperature. A standard hyperfine modulation model (two-site exchange) is proposed and has been added to the simulation routine. The model works especially well for two of the polymers (poly(ethyl acrylate) and poly(methyl d_3-methacrylate), for which activation barriers for rotation are extracted from Arrhenius plots. The model is somewhat successful for poly(ethyl cyanoacrylate) but fails for poly(ethyl methacrylate) and poly(methyl methacrylate). This failure is discussed in terms of radical structure and dynamics and the possibility that jumping between more than two low-energy conformational sites is involved. Disruption of the symmetry of the hyperfine couplings at intermediate temperatures supports this explanation.

Introduction

In two previous papers in this series, we presented conclusive spectroscopic evidence and product analysis results for side chain cleavage as the primary mechanistic event in the photodecomposition of acrylic polymers.[1,2] The process is illustrated for poly(ethyl acrylate) in Scheme 1. Simulation of the time-resolved electron paramagnetic resonance (TREPR) spectra of main chain polymeric radicals such as **1a** was straightforward at high temperatures, using standard techniques and motionally averaged hyperfine coupling constants. All of the data in ref 2 were obtained in the "fast-motion" regime of the polymer.

For most of the acrylic radicals we have studied using TREPR, significant line broadening effects appear as the temperature drops below 90 °C. These effects are present for some transitions but not others, and in several cases the familiar alternating line width pattern is present at lower temperatures. This phenomenon generally appears when hyperfine coupling constants are being modulated, in this case by temperature-dependent conformational motion of the polymer main chain near the radical center. In this paper, these temperature effects will be presented and discussed in terms of motional dynamics of the polymer backbone for five different acrylic main chain polymers, all of which have previously been unambiguously characterized at fast motion.

Dynamic effects have been observed previously in steady state EPR (SSEPR) studies of acrylic polymers. However, it is typically the propagating radical (**1c** in Scheme 1) rather than the main chain radical that is observed in this experiment because of the β-scission rearrangement process. (As explained previously, the TREPR experiment is fast enough to detect radical **1a** before this rearrangement takes place.) In initial studies

Scheme 1

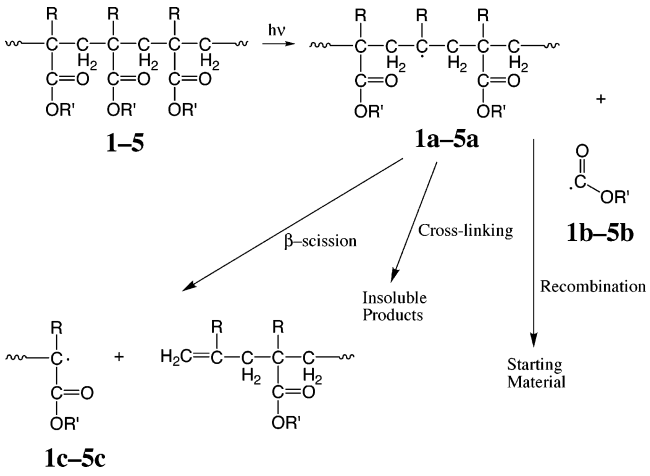

of the photodegradation of these polymers, SSEPR spectra exhibited an unusual nine-line spectrum with alternating line widths of five sharp and four broad lines.[3−6] The spectrum was assigned to the propagating radical **1c**. As a function of temperature, this spectrum changed reversibly to a 13- or 16-line spectrum depending on the available resolution. Four theories have been proposed to account for these findings: One is that there exists a superposition of two or more static conformations of the radical.[7−9] A second theory proposes that the propagating radical exists with a Gaussian distribution of dihedral angles, centered about a single preferred conformation.[10]

A third and most recent theory comes from Matsumoto and Giese, who relied on small molecule model compounds to simulate the propagating radical.[11,12] They suggested that the observed steady state (SSEPR) spectrum was due to a superposition of two conformations of the same radical, one of which would convert reversibly into the other at a given temperature. However, they also assumed that the radical center was

* To whom correspondence should be addressed. E-mail: mdef@unc.edu.

10.1021/ma047801x CCC: $30.25
Published on Web 03/22/2005

pyramidalized, i.e., that it was pure sp^3-hybridized rather than sp^2-hybridized due to steric hindrance. Such an assumption is not supported by the literature on free radicals. There are numerous reports of sterically hindered radicals that are still sp^2-hybridized.[13,14] Only strongly electronegative substituents like fluorine have been found to cause significant deviations toward sp^3 hybridization,[15−17] and there are solid arguments for this phenomenon based on modern electronic structure theory. Extreme pyramidalization of radicals containing only C, H, and O atoms generally occurs only in rigid systems like the adamantyl radical.[18]

Iwasaki[19] invoked a fourth model, hyperfine modulation, to explain the spectra of the propagating radical and were able to simulate their observed 9- and 13-line SSEPR spectra using a set of modified Bloch equations for a two-site exchange model between two conformations. By varying the correlation times of the conformations over an order of magnitude, reasonable fits to the experimental data were obtained.

For main chain polymeric radicals studied here, which are created in solution at room temperature and above, the presence of a superposition of conformations or Gaussian distributions is unlikely. Polymers are known to undergo conformational jumps on the submicrosecond time scale, even in bulk at room temperature.[20−22] Both of the first two theories above require that the radicals be fairly rigid with little (Gaussian distribution) or no (superposition of static conformations) movement around the $C_\alpha-C_\beta$ bond. The polymeric radical studied here is sterically hindered but still conformationally quite flexible; therefore, such a dramatic change in hybridization is not likely. For these reasons we have approached our simulations with the hyperfine modulation model, the details of which we now briefly present.

The alternating line width effect in EPR spectroscopy was discovered independently in the early 1960s by Bolton and Carrington and by Freed, Bernal, and Fraenkel.[23,24] The physical origin of this effect is that the hyperfine couplings fluctuate due to some inter- or intramolecular process. Selective broadening of the lines in the spectrum (in the condition of fast exchange) occurs according to the equation[25]

$$T_2^{-1} = \gamma_e^{\,2}\tau\langle(\delta a)^2\rangle(M_a - M_b)^2 + T_{2,0}^{-1} \qquad (1)$$

where T_2^{-1} is the line width after broadening, γ_e is the gyromagnetic ratio of the electron, M_a and M_b are the nuclear spin quantum numbers of the transitions, and $T_{2,0}^{-1}$ is the contribution to the line width from other mechanisms. The term τ is the correlation time for the exchange process and can be calculated from

$$\tau = \frac{\tau_1\tau_2}{\tau_1 + \tau_2} \qquad (2)$$

where τ_1 and τ_2 are the inverse of the rate constants for jumping the barrier to rotation. The mean-square deviation in the hyperfine splitting is

$$\langle(\delta a)^2\rangle = (1/4)(a_1 - a_2)^2 \qquad (3)$$

where $(a_1 - a_2)$ is the difference between the fast-motion hyperfine coupling constants. An excellent example of a two-site exchange process leading to hyperfine coupling constant modulation is the vinyl radical studied by Sullivan et al.[26] With regard to radicals such as **1a**, an important requirement of this model is that the hyperfine couplings be anticorrelated; i.e., the sum of the hyperfine coupling constants always remains constant.[27]

Chart 1

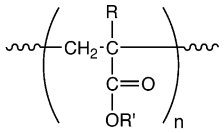

Polymer	Acronym	R	R'
1 Poly(ethyl acrylate)	PEA	H	CH_2CH_3
2 Poly(methyl d_3-methacrylate)	d_3-PMMA	CD_3	CH_3
3 Poly(ethyl cyanoacrylate)	PECA	CN	CH_2CH_3
4 Poly(ethyl methacrylate)	PEMA	CH_3	CH_2CH_3
5 Poly(methyl methacrylate)	PMMA	CH_3	CH_3

The appearance of the spectrum depends on whether the system is undergoing fast or slow motion or is in some intermediate state. These regimes are defined by the correlation times for the two conformations and the difference of the resonance frequencies, $\Delta\omega$, of the two transitions:

$$\tau\Delta\omega < 1 \quad \text{(fast motion)} \qquad (4)$$

$$\tau\Delta\omega \geq 1 \quad \text{(slow motion)} \qquad (5)$$

In the region of fast motion, the correlation time is shorter than the inverse of the difference in resonance frequencies. This will result in one average transition for the two conformers. The opposite holds true for slow motion, where separate and sharp lines for each of the two conformations are observed. We note that in Sakai and Iwasaki's work on the propagating radical[10] the opposite trend was observed. This was interpreted as a crystalline transition that affected the energy barrier.

If the motion of an acrylic polymer radical about the $C_\alpha-C_\beta$ is hindered, then changing the temperature should lead to changes in the appearance of the TREPR spectrum, and this is indeed observed for all of the polymers studied here. Simulation of the complete temperature dependence of TREPR spectra of acrylic polymer main chain radicals should allow information regarding the conformational motion of the polymer in solution to be extracted. By careful analysis of the experimental data, information such as rotational correlation times, spin−lattice relaxation times (T_1), and activation energies for conformational transitions can be derived.

Results and Discussion

The polymers studied in this work are shown in Chart 1. They are all polymers for which the high-temperature (fast-motion) TREPR spectra are simulated to a high level of confidence. The synthesis, sample preparation, polymer characterization, and spectroscopic methods are all described in our earlier publication.[2]

It is instructive to briefly outline our simulation routine: a two-site jump model for hyperfine modulation is incorporated into our standard chemically induced electron spin polarization (CIDEP) simulation program. The spectroscopic and physical features of the model are illustrated in Figure 1. The methyl group hyperfine

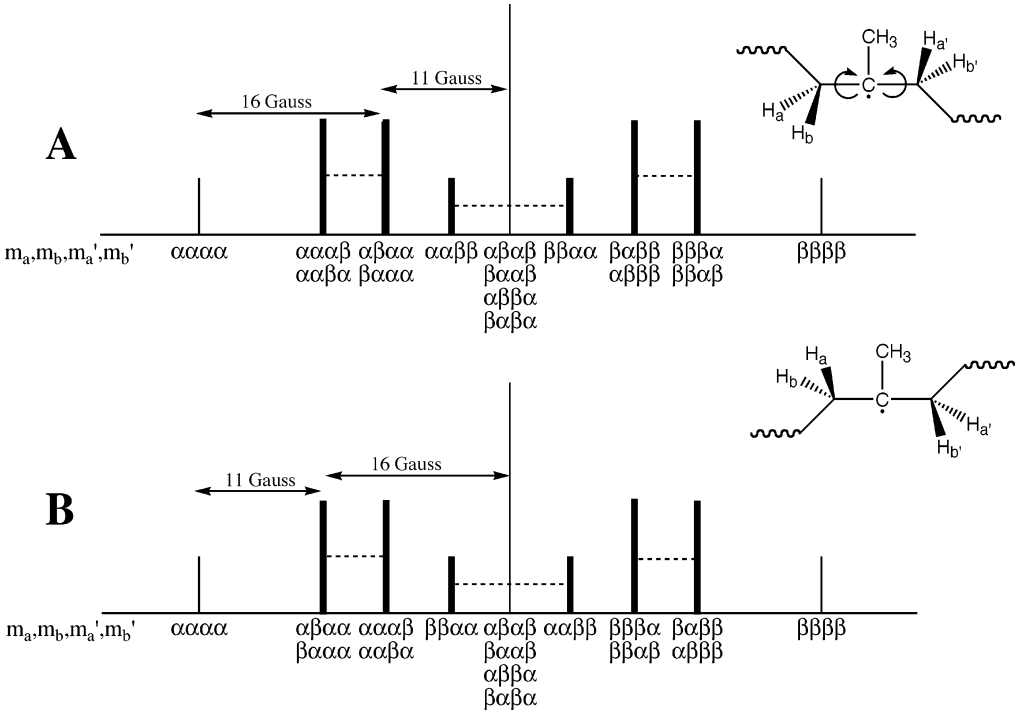

Figure 1. Streamlined view of the hyperfine modulation model used in the simulation program. The methyl group hyperfine couplings have been removed for clarity. The conformational change shown converts one triplet of triplets from the equivalent β-methylene protons on one side of the radical center (H_a, H_b) into their symmetric counterparts on the other side (H_a', H_b'), and vice versa. The nuclear spin quantum numbers representing each transition in each state (A and B) are shown below the transitions in α and β notation. Dashed lines drawn between thick lines show transitions that exchange due to the motion—these lines broaden in the TREPR spectrum. The transitions represented with thin lines remain sharp through the modulation process as their total nuclear spin quantum number does not change during a jump between sites.

coupling constant in PMMA radical **1a** is assumed to be constant for all conformations and therefore is omitted from the figure. It is assumed that one of the two triplets from the β-hyperfines (two diastereotopic H's on either side of the radical center) is being modulated into the second triplet on some time scale, τ. The hyperfine values for H_a and H_a' are exchanging into those for H_b and H_b', and vice versa. This process is shown graphically on the right-hand side of Figure 1. This clearly indicates the anticorrelation of the two triplets. In the first conformation shown in Figure 1A, the stick plot expected from this triplet of triplets is shown with a given set of hyperfine couplings. Below this stick plot, the total nuclear spin quantum numbers for each transition are listed (our notation reads that α represents $m_S = +1/2$ and β represents $m_S = -1/2$). The lines that do not change total spin quantum numbers upon interconversion to the new triplet of triplets are the transitions that remain sharp in the TREPR spectrum. These are indicated with thin lines in the stick plots. Transitions exchanging different total spin quantum numbers are broadened as predicted by eq 1. Specifically exchanged lines are connected with dashed horizontal lines in Figure 1.

Three sets of hyperfine coupling constants were input to the simulation program. The methyl (or α-coupling for PEA) hyperfine coupling constant is assumed to be the same in all conformations and is not considered further. The program is able to calculate the amount of line width added to each transition from β-hyperfine modulation separately for each pair of protons according to eq 1. Values for the correlation time (τ_c) and the hyperfine difference ($a_1 - a_2$) were input as fitting parameters. In all the simulations shown here, the ($a_1 - a_2$) value used was 15.6 G. The program calculates the amount of additional line width based on the change in nuclear spin quantum numbers for each transition. Some of the lines in the spectrum received no additional broadening ($M_1 - M_2 = 0$) as per eq 1. As was noted in the discussion on hyperfine modulation, one of the requirements for the hyperfine modulation mechanism to be active is that the sum of the hyperfine couplings must remain constant. A value of 28 G (approximately the sum of the two fast motion (average) coupling constants) was used for this sum.

Conformational Analysis of Main Chain Acrylic Radicals. With the exception of the α-hyperfine interaction of the backbone H in PEA, all of the hyperfine couplings in the polymeric radicals above result exclusively from β-hyperfine interactions; i.e., they arise from hyperconjugation between the C−H σ-bond and the unpaired electron in the p-orbital. The magnitude of the coupling depends on the dihedral angle θ between the σ-bond and the p-orbital and can be determined quantitatively.[28,29] Scheme 2 shows Newman projections of the polymer down each of the C_α−C_β bonds of the radical produced upon side chain cleavage. The spectral simulations presented below will reveal that at high temperatures the two pairs of methylene proton coupling constants merge to the same values in PMMA and that both of the methylene hyperfine coupling constants differ significantly from the methyl group coupling constant. From the large difference between the PMMA and PEA spectra and the strong tacticity dependence of the PMMA spectra established in our previous paper, it is possible to establish a connection between the stereochemical configuration closest to the radical center and the resulting symmetry relationships in the free radicals.

Scheme 2

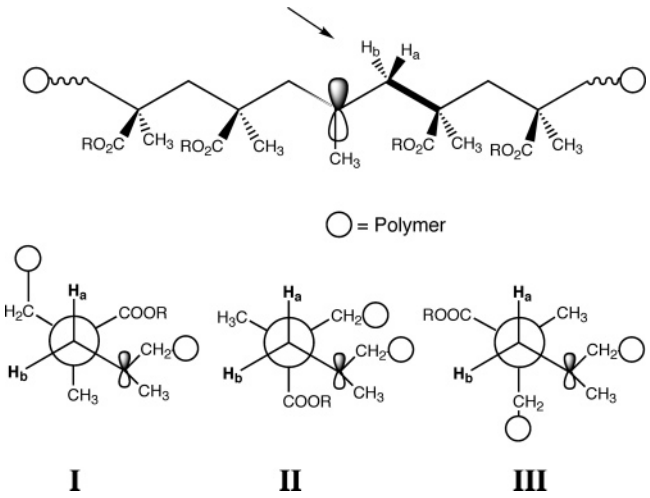

I **II** **III**

The difference in the fast-motion average hyperfine couplings in the simulations of the TREPR spectra of the polymeric radicals from PEMA (**4a**) and PMMA (**5a**) can be qualitatively assessed by considering the relative conformational energies of the polymers in solution. The three staggered Newman projections along one of the $C_\beta-C_\gamma$ bond of the polymeric radical of either PEMA or PMMA are shown in Scheme 2 and are labeled as conformations I, II, and III. While the absolute energies are not known, for qualitative discussion we estimate their relative energies based on the steric bulk of the substituents as $E_{II} \gg E_{III} > E_I$. From some preliminary efforts to model these energetics using force field calculations on short oligomers, we have concluded that long-range macromolecular effects on the energies of the conformers in Scheme 2 may be significant, and a large amount of work remains to be done to accurately model the motional dynamics of these structures.

Continuing qualitatively for the present discussion, each of the conformations in Scheme 2 will be populated at a specific temperature by some mole fraction x_I, x_{II}, or x_{III} of the polymer. The observed fast motion hyperfine coupling constant a_H can be calculated from the equation below if the relative energies (and therefore mole fractions) are known:

$$a_H = x_I a_{HI} + x_{II} a_{HII} + x_{III} a_{HIII} \qquad (6)$$

where a_I, a_{II}, and a_{III} are the hyperfine coupling constants of either H_a or H_b in each of the three conformations in Scheme 2. When the temperature is raised or lowered, the relative populations of the three conformations are altered, which in turn changes the mole fractions of the conformations of interest. This ultimately affects the observed hyperfine coupling constant in the TREPR spectrum. However, in the process we are observing we assume only two conformations participate and that they are equally populated. Below we will present a discussion of the justification of this statement. When the polymer is changed from PMMA to PEMA, the relative energies of the three conformations (and possibly also the barrier heights) are changed. We believe this to be the main reason why the hyperfine coupling constants change from one polymer to the next. In the simulations presented for PMMA, PEMA, and the other polymers studied in this work, the hyperfine couplings remain fairly constant at high temperatures, indicating that the conformational energies of the polymers are somewhat similar but not identical. In fact, our TREPR spectra exhibit a remarkable and unexpected sensitivity to the long-range effects of the side chain substituents.

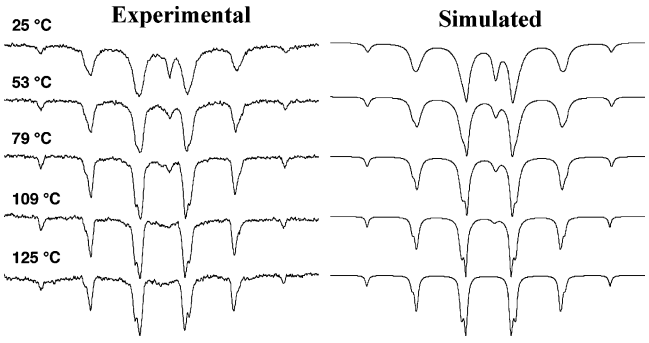

Figure 2. Experimental (left) and simulated (right) TREPR spectra of polymeric radical **1a** from poly(ethyl acrylate) (PEA) in propylene carbonate solution at the temperatures indicated. Sweep width of all spectra is 200 G. The simulation parameters used in each simulation are given in Table 1.

For the present work we assume that the two site model will work and most likely consists of jumping between conformers I and III in Scheme 2, with conformer II being too high in energy to contribute effectively to the mole fraction x_{II} in eq 7 above. High-level computational work at the ab initio level with geometry optimization is being carried out at present on PMMA oligomers in an attempt to model these conformational dynamics quantitatively. Once a more precise model is in place we will use it, together with our TREPR data, to determine the relative energies of the polymer conformations. It will be of great interest to determine the degree of long-range vs short-range structural influence on these dynamics.

A. Poly(ethyl acrylate). Figure 2 shows the temperature dependence of the TREPR spectra of the PEA radical **1a** in propylene carbonate at a variety of temperatures. As the temperature is increased from 25 to 125 °C, the broad inner lines become sharp doublets. The doublets are resolved for the innermost lines at a temperature of 79 °C. At lower temperatures, a singlet slightly to the right of center is observed and is assigned to the oxo-acyl radical **1b**. The rapid decay of this signal is most likely due to fast spin relaxation[30] and perhaps also some chemical decomposition of the radical. The delay time after the laser flash at which these data were collected is 0.9 μs, which is where the maximum intensity of the polymer radical signal is usually observed. The signal from the oxo-acyl radical reaches a maximum $\sim$0.3 μs. As the temperature is increased, the signal from the oxo-acyl radical gradually decreases in intensity, and at 109 °C its signal has disappeared almost completely at this delay time.

The simulations produced for the photolysis of PEA using this modified program are shown on the right side of Figure 2 with the corresponding experimental spectra on the left. The parameters used are given in Table 1. Included in the simulations of the lower temperature spectra, the oxo-acyl radical **1b** can be observed as a sharp singlet. A line width of 3.2 G and a *g*-factor of 2.0008 were used for the simulations of the oxo-acyl radical.

By visual inspection, the simulations are well matched to the experimental data. This is particularly true at the higher temperatures. As the temperature decreases, there are minor deviations in the line shape of the

Table 1. Parameters Used in the Simulation of the Temperature Dependence of TREPR Spectra of Radical 1a (from PEA) Shown in Figure 2

temp (°C)	a_H (G)	a_{CH_2} (G)	a_{CH_2} (G)	line width (G)	$\tau_c \pm 0.2$ (s)
25	21.5	23.3	24.0	3.0	3×10^{-10}
53	21.5	23.3	23.9	2.5	2×10^{-10}
79	21.5	23.5	24.1	2.0	1×10^{-10}
109	21.5	23.5	24.0	1.5	9×10^{-11}
125	21.7	23.5	23.8	1.7	

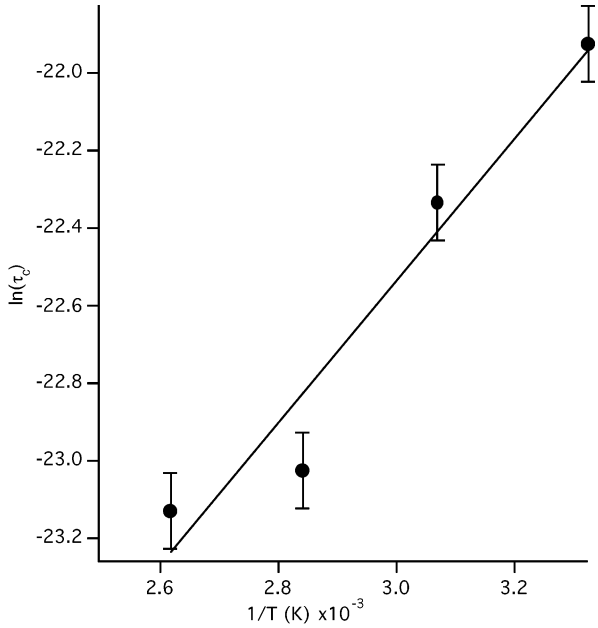

Figure 3. Arrhenius plot for rotational correlation time data from TREPR spectra of polymeric radical **1a**. Dots are the experimental data, and the solid line is the linear fit with $E_a = 15 \pm 2$ kJ/mol.

central two lines of the polymer radical. This is probably due to differences in the hyperfine values used for the β-methylene protons. In these simulations, it was assumed that the hyperfine values remained constant for both pairs of protons. This may not always be the case, as will be seen below for the poly(alkyl methacrylates). Minor variations were necessary to maintain the correct spectral width. The hyperfine coupling constant for the α-proton remained the same at all temperatures, except for the spectrum at 125 °C, where the value increased by 0.2 G. These slight variations most likely reflect the varying contributions of the polymer conformations to the faster motion spectra and therefore slightly different average hyperfine coupling constants. A small amount of increasing natural line width was needed for each line, independent of the modulation process, to best fit these data. This suggests that hyperfine anisotropy may be slightly greater for PEA than for the methacrylates.

The rotational correlation times used in the simulations are also listed in Table 1. The τ_c values are comparable to those found by SSEPR and fluorescence depolarization methods for PMMA.[31−33] The correlation times were used to determine the activation energy of the conformational changes in the polymeric radical of PEA using the Arrhenius equation with the rate constant k equal to $1/\tau_c$. The slope of a plot of $\ln(\tau_c)$ vs $1/T$ will be positive and give the activation energy directly. Figure 3 shows the Arrhenius plot of the correlation times found for the PEA polymeric radical, **1a,** at different temperatures in propylene carbonate. The activation energy determined from the slope of this plot

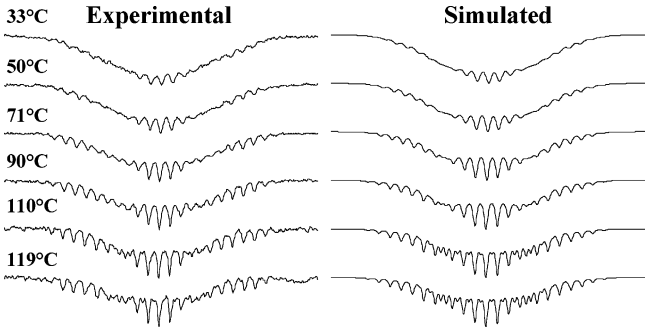

Figure 4. Experimental (left) and simulated (right) TREPR spectra of the polymeric radical **2a** from poly(methyl d_3-methacrylate) in propylene carbonate solution at the indicated temperatures. Sweep width for all spectra is 200 G. Simulation parameters are listed in Table 2.

Table 2. Parameters Used in the Simulation of the Temperature Dependence of TREPR Spectra of Radical 2a (from d_3-PMMA) Shown in Figure 4

temp (°C)	a_D (G)	a_{CH_2} (G)	a_{CH_2} (G)	line width (G)	$\tau_c \pm 0.2$ (s)
33	3.5	15.7	10.3	2.7	2.5×10^{-10}
50	3.5	15.9	10.5	2.2	2.0×10^{-10}
71	3.5	16.1	10.7	1.7	1.0×10^{-10}
90	3.5	16.3	10.9	1.5	7.0×10^{-11}
110	3.5	16.3	10.9	1.4	
119	3.5	16.3	10.9	1.3	

is 15 ± 2 kJ/mol. This value is comparable to those measured for poly(methyl acrylate) by Bullock using spin-labeling methods (19 ± 3 kJ/mol). However, both the value found here and Bullock's are somewhat lower than a value of 23 kJ/mol determined by North using dielectric measurements.[34] This discrepancy is probably a function of the small difference in side chain and solvent. It is known that addition of larger alkyl groups on the ester tail will affect the dynamics of the polymer in solution from NMR experiments. The solvent system is also different for all three of the previous E_a determinations, and activation energies have been shown to vary over 5 kJ/mol in chlorinated solvents alone.[35] Variation in the molecular weight of the three different samples is not likely to be the cause of major differences in the E_a values. In fact, the TREPR spectra of all of these acrylic polymer radicals have, to date, not been dependent on the molecular weight of the polymer. Relaxation of the polymer is not due to end-over-end motions but instead to segmental motions which are not very sensitive to variations in the molecular weight.[32,33] Rotation of the polymer around the $C_\alpha-C_\beta$ bond may also be affected by the presence of the radical center and might be different from that of the nonradical polymer. Overall, the E_a value obtained is certainly of the correct order of magnitude compared to other studies on similar polymer structures.

B. Poly(methyl d_3-methacrylate). The temperature dependence of the TREPR spectra from the deuterated PMMA polymer radical **2a** is shown in Figure 4. The differences between the spectra at the various temperatures are less dramatic than that of the nondeuterated polymer due to the smaller spectral width of the spectra. The spectra again show the alternating line width effect at the lower temperatures. The simulations are shown to the right of the experimental data in Figure 4, and the simulation parameters are presented in Table 2. In all simulations, a value of 3.5 G was used for the hyperfine coupling constant of the CD_3 group because this group is always in fast rotation about the $C_\alpha-C_\beta$

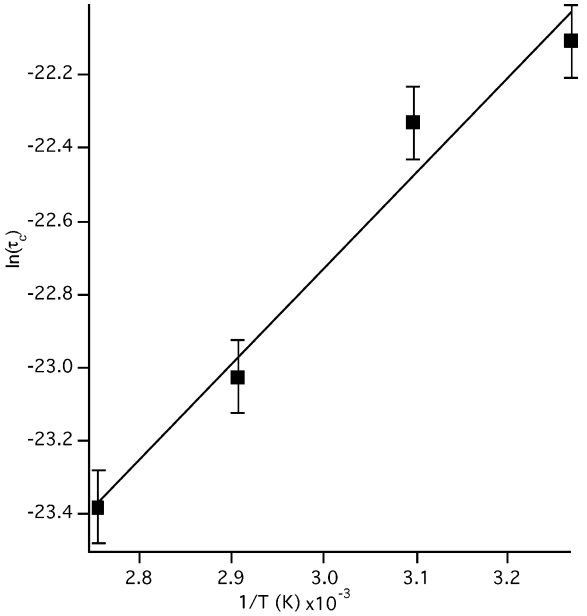

Figure 5. Arrhenius plot for rotational correlation time data from TREPR spectra of polymeric radical **2a**. Squares are the experimental data, and the solid line is the linear fit with $E_a = 22 \pm 2$ kJ/mol.

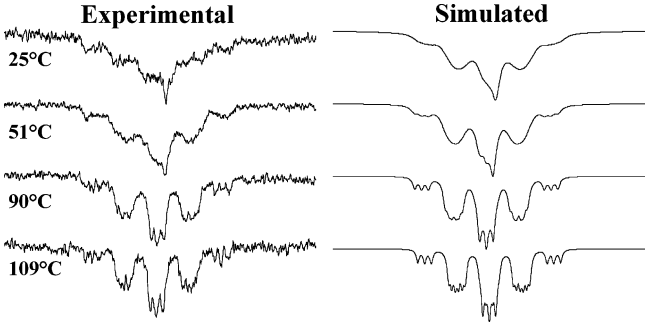

Figure 6. Experimental (left) and simulated (right) TREPR spectra of the polymeric radical **3a** from poly(ethyl cyanoacrylate) (PECA) in propylene carbonate solution at the indicated temperatures. Sweep width of all spectra is 150 G. Simulation parameters are listed in Table 3.

Table 3. Parameters Used in the Simulation of the Temperature Dependence of TREPR Spectra of Radical 3a (from PECA) Shown in Figure 6

temp (°C)	a_N (G)	a_{CH_2} (G)	a_{CH_2} (G)	line width (G)	τ_c (s)
25	3.3	16.5	14.6	6.0	3.0×10^{-10}
51	3.3	16.5	14.6	4.2	2.0×10^{-10}
90	3.3	16.5	14.6	2.3	3.0×10^{-11}
109	3.3	16.3	14.8	2.0	

bond. It would be unexpected for this value to change drastically in our systems. For the spectra obtained at temperatures of 90, 110, and 119 °C, the hyperfine coupling constants are the same. The only difference is the amount of natural line width added into each of the spectra and the presence of hyperfine modulation at 90 °C. Increases in the natural line width of the spectrum will broaden all of the transitions uniformly, while including hyperfine modulation in the simulation program only broadens selected transitions as described above.

For spectra obtained at 110 and 119 °C, additional line width to each transition equally is necessary to simulate the experimental data. As the temperature drops below 100 °C, incorporation of hyperfine modulation becomes necessary to simulate the data. Simply increasing the natural line width for all transitions without addition of hyperfine modulation does not lead to good fits of the experimental data. As in the TREPR of the PEA radical, as the temperature drops the overall line width of all of the transitions increases, and also slight changes in the average hyperfine coupling constants from 90 to 30 °C were observed. The simulated data in Figure 4 give values of τ_c that closely fit a modified Arrhenius plot shown in Figure 5. The activation energy determined from this plot is 22 ± 2 kJ/mol. This value is somewhat higher than that found for the PEA radical, which is not surprising because the addition of a methyl group on the polymer backbone should change the conformational energies and particularly increase the barriers to rotation of the polymer chain in solution.[36]

C. Poly(ethyl cyanoacrylate). To study the effect of main chain substituents on the appearance of the TREPR spectrum, poly(ethyl cyanoacrylate) (PECA) was photolyzed. Figure 6 shows the temperature dependence of the TREPR spectrum of polymeric radical **3a** in propylene carbonate. The high-temperature spectrum (109 °C) was successfully simulated in ref 2. Because of the small hyperfine coupling to the CN nitrogen on the side chain, and the nearly equal values of the β-methylene coupling constants, the two packets immediately adjacent to the center of the spectrum are split into multiplets. As the temperature is decreased, all of the lines in the spectra begin to broaden equally. At room temperature, the signal due to the polymeric radical is little more than an emissive background, and the signal from the oxo-acyl radical appears as a sharp singlet.

It is difficult to conclude whether the TREPR spectra of this polymer are exhibiting hyperfine modulation. There are no lines in the lower temperature spectra that remain sharp throughout the entire temperature range. The right-hand side of Figure 6 shows simulations of the experimental data with the parameters given in Table 3. At 25 and 51 °C, the spectrum of the oxo-acyl radical was included in the simulation. Visually, the simulations of the data obtained at 90 and 109 °C represent good fits to the experimental results. However, at the lower temperatures, the simulated spectra are not fit with unique sets of coupling constants. Large amounts of natural line width had to be added in order to broaden the spectra enough so that the triplet due to the nitrogen atom would not be resolved. This made it difficult to gauge the correct value for τ_c. The error in the rotational correlation time is very large, at least 50−75% of the value listed in Table 3. Because of this large estimated error, a determination of the activation energy for this polymer was not made.

D. Poly(ethyl methacrylate). Figure 7 shows the temperature dependence of the TREPR spectra of the polymeric radical **4a** obtained by photolysis of PEMA in propylene carbonate solution. The lower temperature spectra show the same alternating line width effect at low temperatures as observed with PMMA. The lines in the TREPR spectrum at 42 °C are much broader than in PMMA. This is expected because the PEMA polymer backbone in solution is much stiffer and has slower dynamics than PMMA. It is well-known from NMR[37,38] and fluorescence studies[39] that the dynamics of the ester group (β-relaxation) can couple to the motion of the polymer backbone (α-relaxation) and influence the

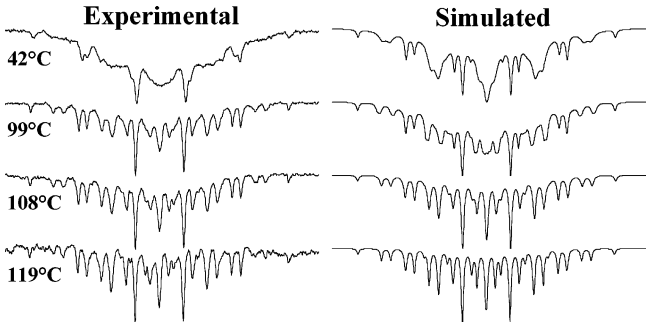

Figure 7. Experimental (left) and simulated (right) TREPR spectra of the polymeric radical **4a** from poly(ethyl methacrylate) (PEMA) in propylene carbonate solution at the indicated temperatures. Sweep width for all spectra is 200 G. Simulation parameters used in each simulation are listed in Table 4.

Table 4. Parameters Used in the Simulation of the Temperature Dependence of TREPR Spectra of Radical 4a (from PEMA) Shown in Figure 7

temp (°C)	a_{CH_3} (G)	a_{CH_2} (G)	a_{CH_2} (G)	line width (G)	τ_c (s)
42	23.1	15.2	11.7	1.5	3.0×10^{-10}
99	23.1	16.0	10.9	1.5	7.0×10^{-11}
108	22.9	16.0	11.4	1.5	5.0×10^{-11}
119	22.9	15.8	11.2	1.3	

α-relaxation rates. Specifically, it has been shown by exchange ^{2}H NMR studies that the relaxation time of PEMA in the solid state above the glass transition temperature is indeed longer than that of PMMA samples.[40] In PMMA, the smaller methyl side chain is highly mobile and cannot couple to the α-relaxation processes of the polymer, and the relaxation of the polymer backbone remains fast. However, the larger ethyl group in PEMA makes the β-relaxation processes of the side chains slower by an order of magnitude and induces anisotropy in the motion of the polymer backbone, decreasing the α-relaxation processes.

Simulations of the TREPR data can be seen in Figure 7 along with the corresponding experimental data using the parameters listed in Table 4. At higher temperatures the simulations reproduce the experimental data very well. However at 42 °C, there are major differences between the experimental and simulated spectra. In the experimental spectrum at this temperature the center line is a strong singlet. This could not be simulated without disrupting the fit of other transitions in the spectrum to unacceptable levels of confidence.

In the experimental spectra, the sharp doublets denoted at the bottom of each experimental data of Figure 7 with brackets have a decreased separation with decreasing temperature. This presented further difficulties in the simulation. As can been seen in Table 4, the hyperfine coupling constants required to reproduce this decreased difference in the 42 °C simulation of Figure 7 are very different from the values used at higher temperatures. While the separation in the doublet in the simulation does not match that of the experimental data exactly, further changes to the hyperfine values result in a central line that was much too intense. When an appropriate value of τ_c is added into the simulation, the resulting spectrum does not resemble the experimental data. The center line of the simulation is more intense than the doublet, which is not observed in any of the room temperature spectra presented to this point. As will be elaborated upon below, the simulations of the PEMA radical **4a** present many of the same difficulties

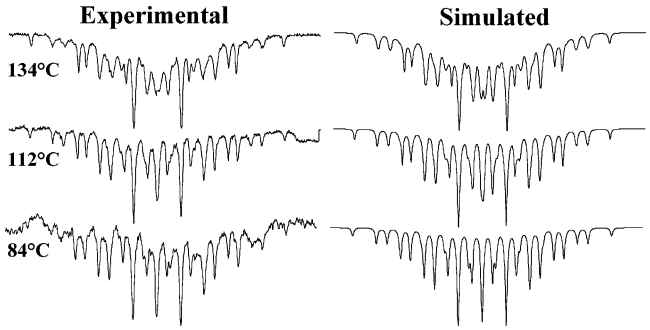

Figure 8. Experimental (left) and simulated (right) TREPR spectra of the polymeric radical **5a** from a-PMMA in propylene carbonate solution at the indicated temperatures. Sweep width of all spectra is 200 G. Simulation parameters are given in Table 5.

Table 5. Parameters Used in the Simulation of the Temperature Dependence of TREPR Spectra of Radical 5a (from a-PMMA) Shown in Figure 8

temp (°C)	a_{CH_3} (G)	a_{CH_2} (G)	a_{CH_2} (G)	a_{CH_2} (G)	a_{CH_2} (G)	line width (G)	τ_c (s)
85	22.9	16.5	10.0	10.8	15.7	1.3	4×10^{-11}
112	22.9	16.5	10.6	11.15	15.95	1.0	2×10^{-11}
134	23.0	16.4	11.3			1.3	

that are encountered in the TREPR spectrum of the PMMA radical.

E. Atactic Poly(methyl methacrylate) (a-PMMA). Figure 8 shows the simulated data for selected TREPR spectra of a-PMMA. The parameters used in the simulations are shown in Table 5. The most striking difference in the simulations of the TREPR spectra of the a-PMMA radical as compared to the other polymeric radicals shown above is the necessity of four different β-hyperfine coupling constants to simulate the spectrum obtained at 112 °C. In other words, the hyperfine coupling constants of the β-methylene protons are no longer the same on each side of the radical. Simulations carried out with only two values of β-hyperfine couplings failed to reproduce the experimental spectrum. What this must mean is the nuclear spin symmetry relationships that work well at high temperatures are disrupted at lower temperatures. More details on this point will be given below.

The simulation of the topmost experimental spectrum shown in Figure 8A is not a good fit. Most noticeably, the central line of the simulation is a narrow doublet, while that in the experimental spectrum is a broad singlet. Attempts to correct this by varying the hyperfine couplings caused larger changes in other parts of the simulation. Increasing the τ_c value had the effect of increasing the intensity of the central line by an unacceptable amount. The line width could not be increased further, as this caused the other peaks in the spectrum to become too broad. At temperatures lower than 80 °C, the simulations break down completely and are not shown. The two-site jump model may not accurately reflect the motion of the polymeric radical in lower temperature solutions. The polymer might be settling into more than one preferred conformation at lower temperatures, causing the TREPR spectrum to become better represented by a superposition of several conformations of the radical.

Scheme 3 helps to amplify this point regarding disruption of symmetry. Here the stereochemistry of the individual radicals produced from isotactic, syndiotactic, and atactic PMMA are shown, as well as the resulting

Scheme 3

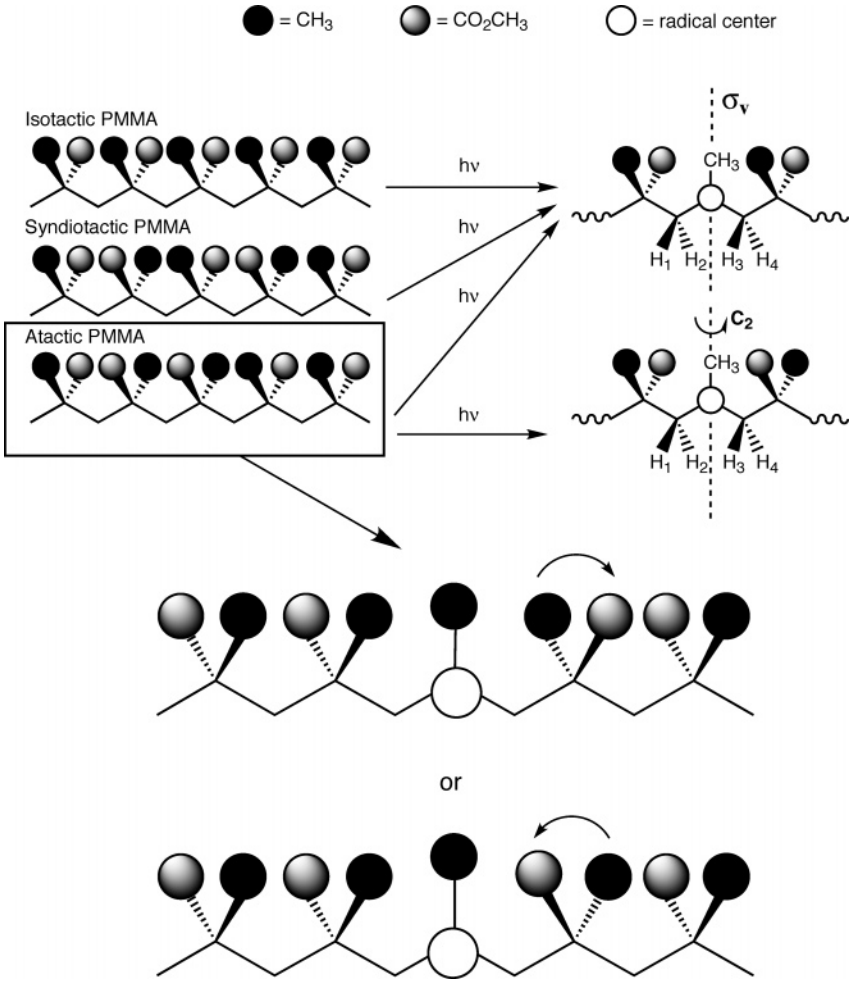

symmetry relationships connecting the nuclei β to the radical center. Particular emphasis is placed on the atactic system, where two different diastereotopic radicals are shown at the bottom of Scheme 3 and enlarged for clarity. Our previous work has shown that the fast motion coupling constants for these two species are identical within experimental limits. However, as the temperature is lowered there is no reason to expect the hyperfines to remain equal. Another way of saying this is that at all times with atactic polymer we are dealing with a superposition of diastereotopic radicals such as the two shown at the bottom of Scheme 3. It is simply fortuitous that they overlap at fast motion. At lower temperatures they would be expected to diverge. In fact, if one considers longer range macromolecular effects, e.g., by considering the stereochemistry of the next two stereogenic centers (one in each direction away from the radical center), it is clear that more than two diastereotopic structures can contribute to the overall TREPR spectrum. This problem does not exist for highly syndiotactic or highly isotactic material, and a detailed study of their temperature dependencies and appropriate molecular modeling may prove more successful. This is the subject of current investigations.

Another possible reason for failing to simulate all of the polymer radicals/spectra/TREPR with the same model is the assumption that the rotational correlation times on either side of the radical center are the same. Although the segmental motion of the polymer has little dependence on molecular weight, there are minor differences with molecular weight, and these could have a large effect on the TREPR spectrum. The rotational correlation times would be the same only if cleavage of the ester side chain occurred near the center of the polymer chain. If the cleavage site was near the end of the polymer chain, then minor differences in the rotational correlation times could have a large effect on the appearance of the TREPR spectrum. The polymer chains are also quite polydisperse, and if the radicals were produced on chains of widely different molecular weight, then the τ values of the two radicals would be different. It is only fortuitous that the hyperfine coupling constants of the high-temperature TREPR spectra are the same on either side of the radical. This is due to the high temperatures and the fast interconversion between the different conformations of the PMMA radical and the fact that the stereochemical differences are manifested at carbon atoms well removed from the radical center.

It is also possible that the wrong dynamic model is being used or that there is combination of models that must be used to fit the experimental data at lower temperatures. It seems likely that, even without considering the stereochemical issues discussed above, there is a superposition of radical conformations that exists in equilibrium at lower temperatures. This is supported by results we have obtained for the polymeric radical from PFOMA at high temperatures and also at low temperatures for poly(adamantyl methacrylate). In these systems broad line widths in the TREPR transitions for the main chain polymers were observed.[41] Another indication that there is a superposition of

conformations comes from the TREPR spectra of the main chain polymeric radical of PMMA measured at close to 0 °C. These spectra are also very broad and featureless. However, previous work from our laboratory has shown that averaging multiple simulations without hyperfine modulation does not reproduce the experimental spectra.[42] Future work will include combining the two models and investigating other models (e.g., three- or four-site jump models) in order to produce accurate simulations.

Finally, it is worthwhile to note that there is no reason to expect PMMA and d_3-PMMA to have exactly the same conformational dynamics. There are many reports in the literature of substantial isotope effects on polymer physical properties. In particular, the works of Bates et al.[43] and Cukier et al.[44] show that rotational dynamics in polybutadienes and polyethylenes, respectively, can show significant changes upon deuteration. This can be simply due to the larger van der Waals radii of the methyl groups in d_3-PMMA, although there may be more subtle stereoelectronic effects as well. The samples used here were of similar chain length, and although there was a slight difference in polydispersity between the protonated and deuterated samples, we have never observed differences in any of our spectra that could be attributed solely to molecular weight changes (down to about $M_w = 10$K for PMMA). The dynamic effects we observe are clearly long range, but not long enough for molecular weight to play a large role. Currently, we are attempting to address this issue by selectively synthesizing known-chain length oligomers of both polymers. This will be the subject of a future publication.

Summary and Outlook

Simulations of the temperature dependence of the TREPR spectra for PEA and d_3-PMMA radicals using a two-site jump model for hyperfine modulation have returned reasonable values for the activation parameters for conformational motion in these polymers. The numbers compare favorably with values determined by NMR and SSEPR methods. For PMMA and PEMA our model was not successful. While the line positions and general line width features could be reproduced, the relative intensities of the transitions were not. It is clear that the simulations of the TREPR spectra shown for the photolysis of PMMA and PEMA do not accurately reflect the experimental data.

Future work to determine whether the position of the cleavage site along the polymer chain has an effect on the rotational correlation time will include photolysis of low molecular weight and oligomeric PMMA. The TREPR spectra of these systems will be compared to those of the large molecular weight polymer. If the spectra of the low molecular weight and oligomeric PMMA are sharp and easily simulated, then differences in the rotation correlation times on either side of the chain will have to be incorporated into the simulation program.

Experimental Section

A complete description of the TREPR apparatus, polymer synthesis, and sample descriptions is given in our previous papers,[1,2] and a summary is provided as Supporting Information to this paper.

Acknowledgment. We thank the Rohm and Haas Co. for polymer samples and the National Science Foundation for their continued strong support of our program (Grant CHE-0213516).

Supporting Information Available: Summary of experimental details. This material is available free of charge via the Internet at http://pubs.acs.org.

References and Notes

(1) McCaffrey, V. P.; Forbes, M. D. E. *Macromolecules* **2005**, *38*, 3334.
(2) Harbron, E. J.; McCaffrey, V. P.; Xu, R.; Forbes, M. D. E. *J. Am. Chem. Soc.* **2000**, *122*, 9182.
(3) Abraham, R. J.; Melville, H. W.; Ovenall, D. W.; Whiffen, D. H. *Trans. Faraday Soc.* **1958**, *54*, 1133.
(4) Doetschman, D. C.; Mehlenbacher, R. C.; Cywar, D. *Macromolecules* **1996**, *29*, 1807.
(5) Kamachi, M.; Kohno, M.; Liaw, D. J.; Katsuki, S. *Polym. J.* **1978**, *10*, 69.
(6) Tian, Y.; Zhu, S.; Hamielec, A. E.; Fulton, D. B.; Eaton, D. R. *Polymer* **1992**, *33*, 384.
(7) Sugiyama, Y. *Bull. Chem. Soc. Jpn.* **1998**, *71*, 1019.
(8) Harris, J. A.; Hinojosa, O.; Arthur, J. C. *J. Polym. Sci., Polym. Sci. Ed.* **1973**, *11*, 3215.
(9) Ingram, D. J. E.; Symons, M. C. R.; Townsend, M. G. *Trans. Faraday Soc.* **1958**, *54*.
(10) Iwasaki, M.; Sakai, Y. *J. Polym. Sci., Part A-1* **1969**, *7*, 1749.
(11) Spichty, M.; Giese, B.; Matsumoto, A.; Fischer, H.; Gescheidt, G. *Macromolecules* **2001**, *34*, 723.
(12) Matsumoto, A.; Giese, B. *Macromolecules* **1996**, *29*, 3758.
(13) Hesse, C.; Roncin, J. *Mol. Phys.* **1970**, *19*, 803.
(14) Griller, D.; Ingold, K. U.; Krusic, P. J.; Fischer, H. *J. Am. Chem. Soc.* **1978**, *100*, 6750.
(15) Beveridge, D. L.; Dobosh, P. A.; Pople, J. A. *J. Chem. Phys.* **1968**, *48*, 4802.
(16) Fessenden, R. W. *J. Phys. Chem.* **1967**, *71*, 74.
(17) Morokuma, K.; Pedersen, L.; Karplus, M. *J. Chem. Phys.* **1968**, *48*, 4801.
(18) Rhodes, C. J.; Walton, J. C.; Della, E. W. *J. Chem. Soc., Perkin Trans. 2* **1993**, *11*, 2125.
(19) Iwasaki, M. S. *J. Polym. Sci., Part A-1* **1969**, *7*, 1537.
(20) Bendler, J. T.; Yaris, R. *Macromolecules* **1978**, *11*, 650.
(21) Inoue, Y.; Konno, T. *Makromol. Chem.* **1978**, *179*, 1311.
(22) Ono, K.; Sasaki, T.; Yamamoto, M.; Yamasaki, Y.; Ute, K.; Hatada, K. *Macromolecules* **1995**, *28*, 5012.
(23) Bolton, J. R.; Carrington, A. *Mol. Phys.* **1962**, *5*, 161.
(24) Freed, J. H.; Fraenkel, G. K. *J. Chem. Phys.* **1963**, *39*, 326.
(25) Fraenkel, G. K. *J. Phys. Chem.* **1967**, *71*, 139.
(26) Sullivan, P. D.; Bolton, J. R. *Adv. Magn. Reson.* **1970**, *4*, 39.
(27) Bubnov, N. N.; Solodovnikov, S. P.; Prokof'ev, A. I.; Kabachnik, M. I. *Russ. Chem. Rev.* **1978**, *47*, 549.
(28) Heller, C.; McConnell, H. M. *J. Chem. Phys.* **1960**, *32*, 138.
(29) Carrington, A.; McLachlan, A. D. *Introduction to Magnetic Resonance*; Harper & Row: New York, 1967.
(30) Paul, H. *Chem. Phys. Lett.* **1975**, *32*, 472.
(31) Tsay, F.-D.; Gupta, A. *J. Polym. Sci., Part B* **1987**, *25*, 855.
(32) Sasaki, T.; Nawa, K.; Yamamoto, M.; Nishijima, Y. *Eur. Polym. J.* **1989**, *25*, 79.
(33) Bullock, A. T.; Cameron, G. G.; Krajewski, V. *J. Phys. Chem.* **1976**, *80*, 1792.
(34) North, A. M. *Chem. Soc. Rev.* **1972**, *1*, 49.
(35) Spyros, A.; Dais, P.; Heatley, F. *Macromolecules* **1994**, *27*, 6207.
(36) Fytas, G.; Meier, G.; Patkowski, A.; Dorfmüller, T. *Colloid Polym. Sci.* **1982**, *260*, 949-.
(37) Kulik, A. S.; Beckham, H. W.; Schmide-Rohr, K.; Radloff, D.; Pawelzik, U.; Boeffel, C.; Spiess, H. W. *Macromolecules* **1994**, *27*, 4746.
(38) Schmidt-Rohr, K.; Kulid, A. S.; Beckham, H. W.; Ohlemacher, A.; Pawlzid, U.; Boeffel, C.; Spiess, H. W. *Macromolecules* **1994**, *27*, 4733.
(39) Saski, T.; Arisawa, H.; Yamamoto, M. *Macromolecules* **1991**, *23*, 103.
(40) Kuebler, S. C.; Schaefer, D. J.; Boeffel, C.; Pawelzik, U.; Spiess, H. W. *Macromolecules* **1997**, *30*, 6597.
(41) McCaffrey, V. P.; Harbron, E. J.; Forbes, M. D. E., submitted to *J. Phys. Chem. B*.
(42) Harbron, E. J. Ph.D. Thesis, University of North Carolina at Chapel Hill, Chapel Hill, NC, 1999.
(43) Bates, F. S.; Keith, H. D.; McWhan, D. B. *Macromolecules* **1987**, *20*, 3065.
(44) Cukier, R.; Natarajan, K.; Samulski, E. T. *Nature (London)* **1978**, *275*, 527.

MA047801X